Journal of Materials Chemistry

www.rsc.org/materials

Volume 20 | Number 13 | 7 April 2010 | Pages 2481–2692

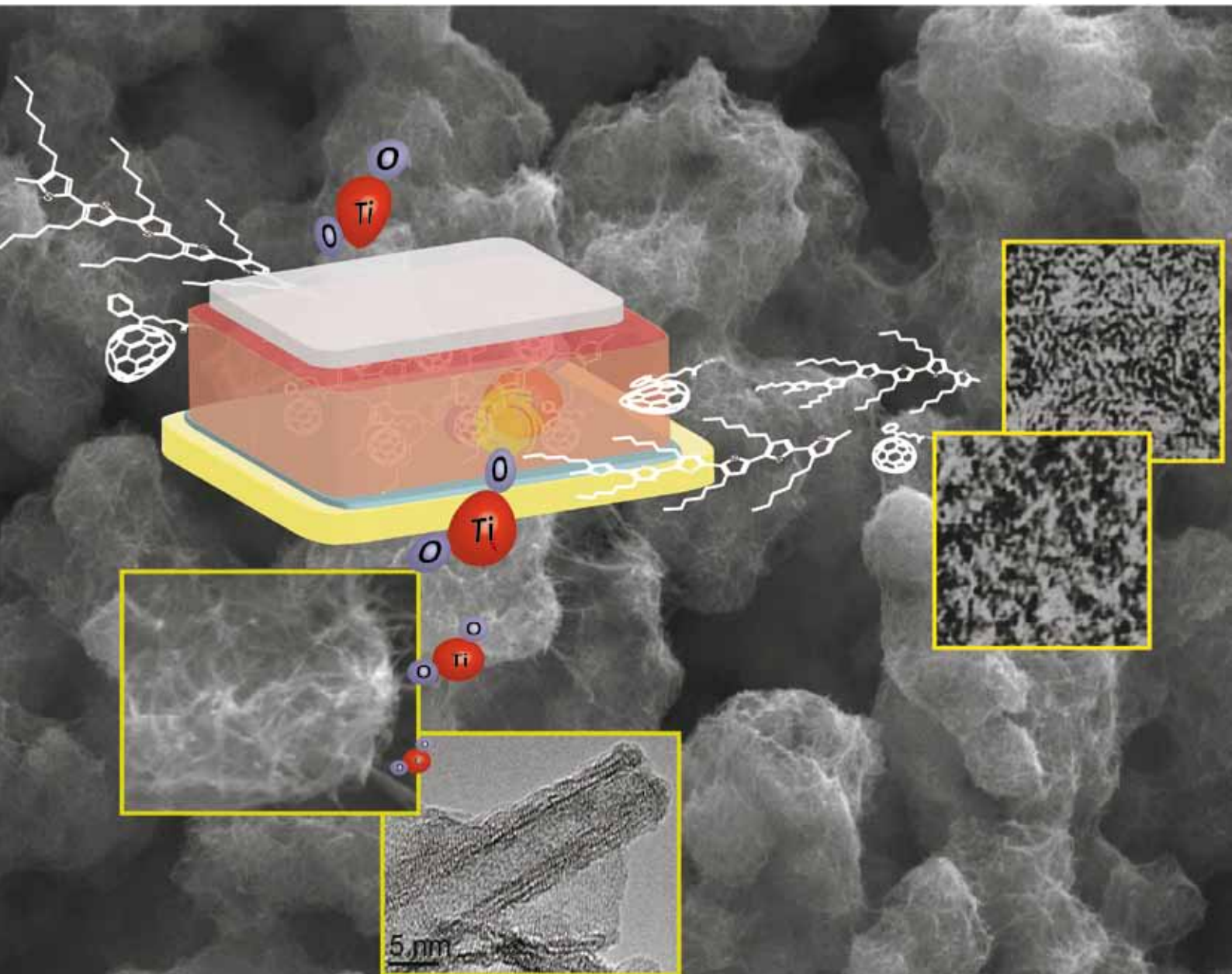

Interface Engineering of Organic and Molecular Electronics

ISSN 0959-9428

RSC Publishing

P3HT:PCBM polymer solar cells with TiO_2 nanotube aggregates in the active layer†

Pinyi Yang, Xiaoyuan Zhou, Gongzhong Cao and Christine K. Luscombe*

Received 20th October 2009, Accepted 5th January 2010
First published as an Advance Article on the web 22nd January 2010
DOI: 10.1039/b921758d

P3HT:PCBM polymer solar cells with a very small amount of TiO_2 nanotube aggregates (0.002 mol per 100 mL) in the active layer have been fabricated. Although in dye-sensitized solar cells nanotube aggregates have been shown to increase light absorption of devices, it was found that TiO_2 nanotube aggregates reduced the absorbance of the active layer in our case. However, its positive role on the charge collection and transportation maintained the EQE the same as a conventional P3HT:PCBM device and improved the electron mobility from 5.71×10^{-5} cm^2 V^{-1} s^{-1} to 7.22×10^{-5} cm^2 V^{-1} s^{-1}. The final devices showed a 15% increase in power conversion efficiency compared to conventional P3HT:PCBM devices. The effects of TiO_2 nanotube aggregates on the morphology of the active layer were studied by AFM.

Introduction

Ever since conjugated polymers were found to be able to convert light into electricity,[1,2] it has attracted a lot of interest because of the possibility of creating a cheaper and cleaner source of energy compared to existing technologies. Due to its cost and solubility, a large amount of expense can be cut to fabricate solar cells from organic materials compared to inorganic materials.[3–6] However, a key issue of organic photovoltaics (OPVs) is the low efficiency. At least 10% power conversion efficiency should be reached to make them commercially competitive.[7] The main obstacle is the exciton mechanism of the conjugated polymer—after absorbing light, excitons (pairs of a hole and an electron) are generated, which can only diffuse around 20 nm.[8]

One way to overcome the exciton diffusion is to apply the bulk heterojunction structure.[9–11] This structure of the active layer can be easily achieved by spin coating a blend solution of electron donor (conjugated polymer) and acceptor (usually a fullerene derivative). Because of the different chemical structures of the two species, they will separate into two phases within the film.[12] Hence, the bulk heterojunction structure forms within the active layer. During this process, the size of the phase separation and morphology of active layer can be controlled by using different solvents[13,14] and by controlling the solution evaporation rate.[15,16] It has also been found that the morphology of the active layer can be further tuned by the thermal treatment near the glass transition temperature of the conjugated polymer.[15,17,18] All these methods are aimed to tailor the active layer architecture into optimal condition for exciton diffusion and separation.

The most commonly used combination of electron donor and acceptor in the active layer is poly(3-hexylthiophene) (RR-P3HT; P3HT) and [6,6]-phenyl-C_{61}-butyric acid methyl ester (PCBM). The study of the optimal phase separation and morphology as well as the fabrication method has been pursued by many research groups. Besides the methods above, recently, high boiling additives[19] and ordered TiO_2 nanotubes[20,21] have also been applied to affect the active layer morphology. Infiltrating the P3HT:PCBM solution into the ordered TiO_2 nanotubes[22] which can be controlled precisely in size, excitons have an increased probability to reach the interface within its diffusion length (~20 nm). As a result, charge carriers can be more effectively generated and collected in such devices. However, the infiltration is always a big problem in utilizing such a template in the nanometre scale. Introducing the ordered TiO_2 template also increases both the cost and difficulty of the fabrication. Replacing the PCBM inside the active layer is another way to utilize these inorganic oxides nanostructures. Aligned ZnO nanofibers[23] or nanowires,[24] as well as aligned[25,26] or free TiO_2 nanorods,[27] and nanostructured TiO_2 have been utilized in conjunction with either P3HT or MEH-PPV. However, the device performance in these devices is not as efficient as P3HT:PCBM cells. Here, we introduce TiO_2 nanotube aggregates by simply mixing them with P3HT:PCBM solution during fabrication process. The final devices show a 10–20% efficiency increase compared to control group.

Experiment

Material preparation

Commercial grade, nanosize TiO_2 (Degussa Aeroxide P25) was a gift from Degussa Corp. (Parsippany, NJ) and used without any purification or treatment. Degussa Aeroxide P25 powder (1.0 g) was added into a 40 mL aqueous solution of 10 M sodium hydroxide. After sonication for 30 min, the resulting suspension was put into a Teflon-lined autoclave and heated to 160 °C for 24 h. The product was then washed by HCl solutions (0.1 M) followed by centrifugation. This acid washing was repeated three times. After that, the HCl washed samples were washed with ethanol five times to form nanotube structures. Finally the

Department of Material Science and Engineering, University of Washington, Box 352120, Seattle, WA, 98195, USA. E-mail: luscombe@u.washington.edu

† This paper is part of a themed issue of *Journal of Materials Chemistry* on Interface engineering of organic and molecular electronics, guest edited by Alex Jen.

nanotubes were heat treated in air at 500 °C for 2 h. More details of synthesis and final TiO_2 nanotube aggregates structure can be found in ref. 28. XRD (Fig. 1(e)) shows that stoichiometric TiO_2 in the anatase form is created.

Device fabrication

The ITO-coated glass substrates (15 Ω m^{-2}) were cleaned in an ultrasonic bath with detergent, deionized (DI) water, acetone and isopropyl alcohol. Substrates were then taken out and dried under N_2 flow followed by air plasma treatment for 15 min. A hole-transport layer of poly(3,4-ethylene-dioxylene thiophene): poly(styrene sulfonic acid) (PEDOT:PSS, Clevios P VP Al 4083) was spin-coated onto the ITO surface from its aqueous solution (40 nm thick). The films were baked at 140 °C for 10 min before being transferred into an argon-filled glove box. The chlorobenzene solution, which contained 25 mg mL^{-1} P3HT (purchased from Reike Metal, Sepiolid P100) and 15 mg mL^{-1} PCBM (purchased from American Dye Source Inc. ADS61BFB), was stirred inside the glove box for at least 3 h at 60 °C. The active layer of control devices was achieved by directly spin coating the P3HT:PCBM solution to form a 140 nm thick layer. For devices with TiO_2 nanotube aggregates, 0.002 mol per 100 mL aggregates were added into the solution and sonicated for 30 min to disperse the aggregates first. Then, this solution was kept stirring before it was spin-coated onto the PEDOT:PSS to achieve the same thickness active layer as the control group. Subsequently, all the devices were transferred into a deposition chamber inside the glove box and 1 nm of LiF and 100 nm of Al were thermally evaporated under a vacuum of 2×10^{-6} Torr to form circular electrodes with radii of 1 mm. Finally, the devices were completed by annealing at 150 °C for varying times in order to control the morphology of the active layer.

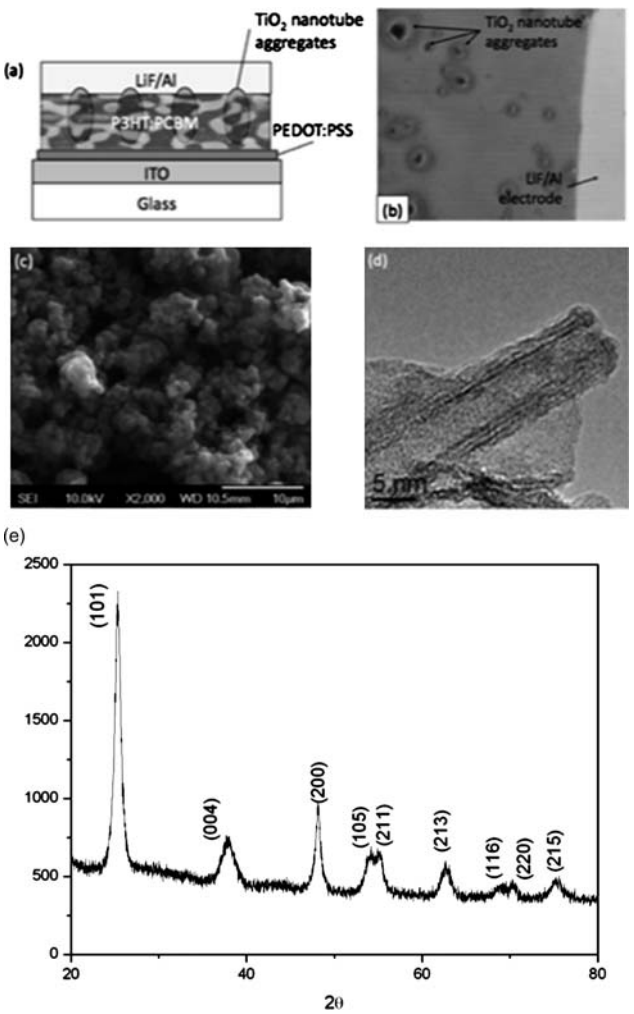

Fig. 1 (a) Schematic diagram of a device structure of solar cell with TiO_2 nanotube aggregates doped active layer. (b) Optical microscope image of surface of solar cell with TiO_2 nanotube aggregates (×500). (c) SEM image of TiO_2 nanotube aggregates. (d) TEM image of a TiO_2 nanotube inside the aggregates. (e) XRD of TiO_2 nanotubes.

Device characterization

The *J–V* characteristics of the solar cells were tested in air using a Keithley 2400 source measurement unit, and an Oriel Xenon lamp (450 W) coupled with an AM1.5 filter was used as the light source. The light intensity was calibrated with a calibrated standard silicon solar cell with a KG5 filter which is traced to the National Renewable Energy Laboratory and a light intensity of 100 mW cm^{-2} was used in all the measurements in this study. Devices parameters were obtained by taking the average of at least 20 samples for each processing condition. The series resistance and parallel resistance were calculated from the inverse of the slope of the *J–V* curve at 1 V and 0 V, respectively. External quantum efficiency (EQE) was measured using an Oriel Cornerstone 130 1/8m Monochromator with the same light source in the *J–V* characteristics. AFM images were taken on a Veeco multi-mode AFM with a nanoscope III controller in tapping mode. The AFM images were taken from actual devices fabricated for measurement of solar performance. Electron-only SCLC devices were fabricated according to the above procedure but the polymers were spin-coated on thermally deposited 100 nm Al instead of PEDOT:PSS.

Results and discussion

Fig. 1(a) illustrates a simplified structure of a solar cell with TiO_2 nanotube aggregates. From the scanning electron microscope (SEM) image of the TiO_2 nanotube aggregates (Fig. 1(c)), it can be seen that it is formed by a large number of TiO_2 nanotubes with a dimension of approximately 10 nm in diameter (Fig. 1(d)). Because the size of aggregates (300–600 nm in diameter) is larger than the thickness of a P3HT:PCBM film (140 nm), they will cause bumps on the surface in the active layer around them. This means that the surface roughness of film will be increased by adding in TiO_2 nanotube aggregates. The optical microscope image of the films (Fig. 1(b)), as well as the AFM images confirm the increase in roughness of the films with and without TiO_2 nanotube aggregates (Fig. 2(a)–(c)). For the conventional film (Fig. 2(a)), the surface is very smooth having a root mean average (rms) roughness of only 0.63 nm. But for the film with TiO_2 nanotube aggregates, the rms roughness of the film increases especially in the area close to the aggregates. In the area some distance away from the aggregates, the rms roughness is a little higher than the normal film reaching 0.95 nm (Fig. 2(b)), while

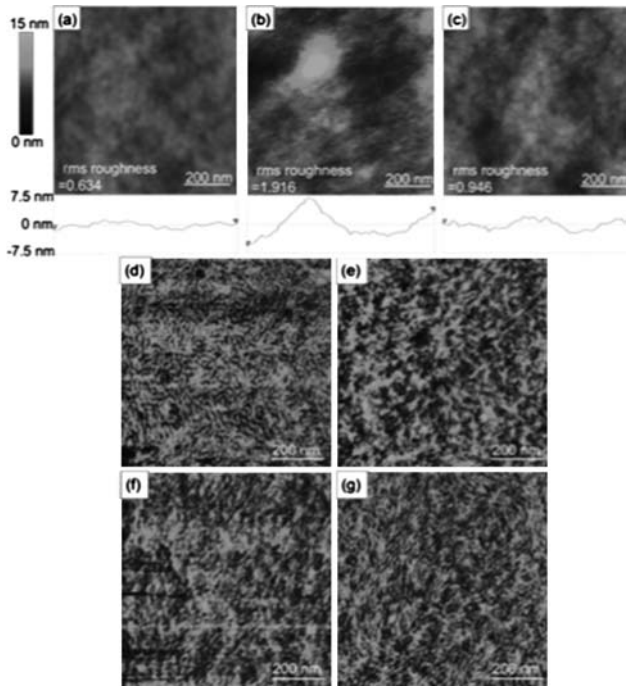

Fig. 2 (a) AFM images of normal P3HT:PCBM active layer; AFM images of active layer with TiO_2 nanotube aggregates, (b) near an aggregate, and (c) some distance from an aggregate. Phase image of P3HT:PCBM film with TiO_2 nanotube aggregates annealed at 150 °C for 5 min, (d) near an aggregate, (e) some distance away from an aggregate; annealed for 9 min, (f) near an aggregate, and (g) some distance away from an aggregate.

this value jumps to 1.92 nm (Fig. 2(c)) when scanning around a medium size TiO_2 nanotube aggregate. Furthermore, in Fig. 1(b), the optical microscope image of the actual film shows that due to the poor control we had during processing, the size and distribution of the TiO_2 nanotube aggregates were not very uniform. Surprisingly, the final devices showed little shorting.

The *J–V* curves of the best control device (annealed for 9 min) and the best devices with the TiO_2 nanotube aggregates annealed for 5 and 9 min are shown in Fig. 3. The power conversion

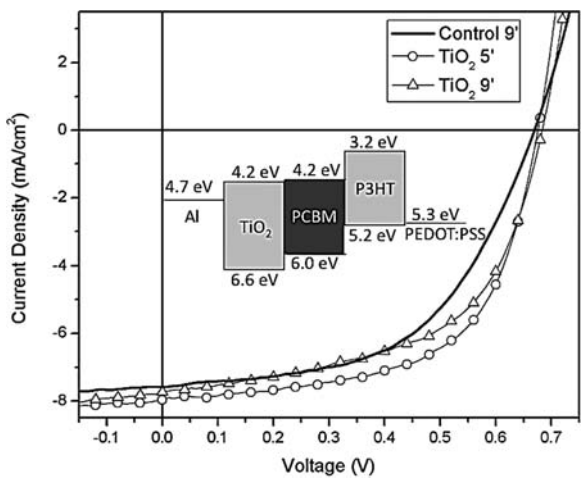

Fig. 3 *I–V* curve of devices with normal active layer and active layer with 0.002 mol per 100 mL TiO_2 nanotube annealed by different time at 150 °C.

efficiency (PCE) of the control sample is 2.8%. Under the same annealing conditions, efficiency of device with TiO_2 nanotube aggregates increased to 3.0%. Moreover, for devices modified by TiO_2 nanotube aggregates, even higher performance was reached by annealing for 5 min, with $V_{oc} = 0.68$ V, $J_{sc} = 8.0$ mA cm^{-2}, FF = 0.60, PCE = 3.2%. Compared to the control sample, the PCE value increased by 15%. In Fig. 3, it can be seen that the values of J_{sc} and V_{oc} of all three devices were almost the same as each other. The 15% increase in device efficiency can be attributed to the increase in the FF in the TiO_2 containing samples, which is indicated by the area between the coordinate axis and the *J–V* curve.

The change in device parameters was more clearly revealed by the summary of the average device performance in both types annealed from 4 to 10 min (Table 1 and Fig. 3). Again, the values of V_{oc} and J_{sc} (Fig. 4(a)) remained almost the same after adding TiO_2 nanotube aggregates, except the maximum J_{sc} of TiO_2 nanotube aggregates containing device appeared at 5 min annealing time. We believe that this early optimization of short current may be a result of the quicker phase change near the TiO_2 nanotube aggregates due to the higher thermal conductivity of TiO_2 compared to polymers. As a result, both morphologies of the two regions can be tuned by controlling the annealing time. Because the region near the TiO_2 nanotube aggregates was heated faster than the rest of the film, the phase separation around the aggregates reached the optimal morphology after only 5 min. As shown in AFM phase images (Fig. 2(d)), after annealing for only 5 min, the area adjacent to the TiO_2 nanotube aggregates formed features which were approximately 20 nm in size (most suited for exciton dissociation), while a longer time (9 min) was needed to optimize for the regions further away from the TiO_2 aggregates (Fig. 2(g)). After 9 min of annealing, the feature size of the area near the TiO_2 nanotube aggregates has already exceeded the optimal morphology with features with sizes greater than 100 nm appearing (Fig. 2(f)).

Since there was little difference in the values of V_{oc} and J_{sc}, the enhancement in the PCE of TiO_2 nanotube aggregates solar cell is mainly due to the increase in the FF. It can be seen in Fig. 4(b) that the FF of TiO_2 nanotube aggregates devices was always higher than the control group. This increase in FF can be traced to the decrease in the serial resistance (R_{serial}) of the active layer (Table 1 and Fig. 4(c)). After adding in TiO_2 nanotube aggregates the R_{serial} values were reduced to half compared to the control group. The shunt resistance (R_{shunt}) decreased as well but to a lesser extent. As the surface roughness of the films plays a minor role in the device efficiency enhancement,[17] this dramatic reduction in serial resistance may be attributed to the TiO_2 nanotube aggregates' ability to improve the charge transportation through the active layer. In order to investigate the increase in the PCE caused by the TiO_2 aggregates, we decided to study the different steps involved in device performance, namely light absorption, charge dissociation, charge transport and charge collection. It was originally expected that the TiO_2 aggregates may increase the light absorption since a similar effect had previously been observed for dye-sensitized solar cells.[29] By comparing the absorption spectrum (Fig. 5(a)) of films with and without TiO_2 nanotube aggregates after annealing, it was found that rather than helping absorb more light, the annealed solar cells with TiO_2 nanotube aggregates absorb less in the range of

Table 1 Summary of devices parameters of normal active layer and active layer with 0.002 mol per 100 mL TiO_2 nanotube annealed by different time at 150 °C

Devices[a]	Anneal time/min	V_{oc}/V (≤ +0.01 V)	J_{sc}/mA cm^{-2}	FF	PCE (%)	R_{shunt}/Ω cm^{-2}	R_{serial}/Ω cm^{-2}
Control	4	0.66	7.2 ± 0.5	0.50	2.4 ± 0.2	790	4.7
	5	0.67	7.0 ± 0.3	0.55	2.7 ± 0.1	790	4.7
	6	0.66	7.6 ± 0.3	0.52	2.6 ± 0.2	680	4.3
	8	0.67	7.4 ± 0.3	0.53	2.7 ± 0.1	810	4.5
	9	0.67	7.4 ± 0.2	0.55	2.7 ± 0.0	830	3.8
	10	0.68	7.6 ± 0.4	0.51	2.6 ± 0.2	690	5.0
0.002 mol per 100 mL TiO_2 nanotube	4	0.67	6.8 ± 0.4	0.56	2.6 ± 0.2	590	3.4
	5	0.67	7.9 ± 0.2	0.58	3.1 ± 0.1	590	2.4
	6	0.68	7.4 ± 0.5	0.54	2.7 ± 0.2	560	3.7
	8	0.68	7.3 ± 0.2	0.56	2.8 ± 0.1	540	3.3
	9	0.68	7.5 ± 0.3	0.57	2.9 ± 0.1	620	2.8
	10	0.67	7.3 ± 0.5	0.55	2.7 ± 0.2	600	3.3

[a] Device parameters were taken to be the average of at least 20 samples.

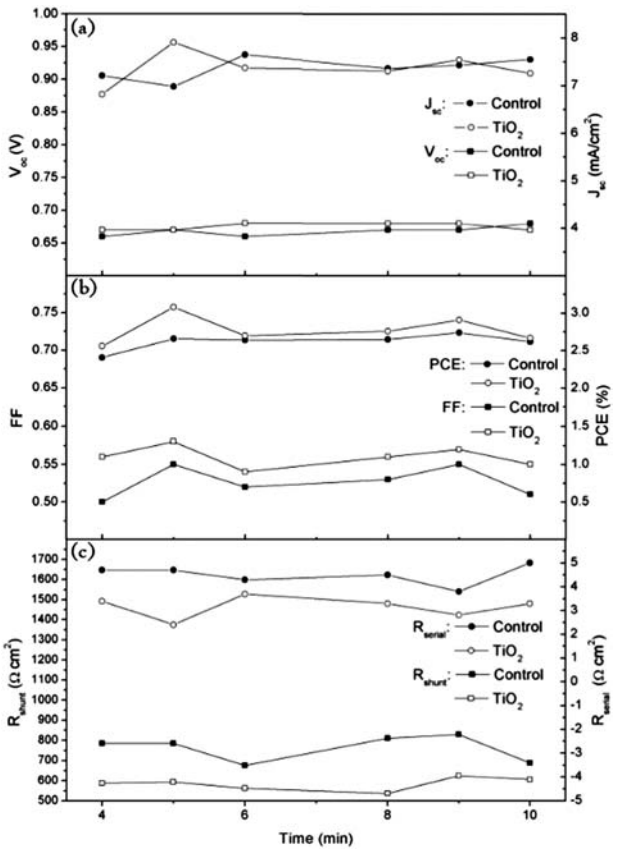

Fig. 4 Device parameters plotted as a function of annealing time at 150 °C for solar cell with and without TiO_2 nanotube aggregates: (a) open circuit voltage (V_{oc}) and short circuit current density (J_{sc}); (b) fill factor (FF) and power conversion efficiency (PCE); and (c) serial resistance (R_{serial}) and shunt resistance (R_{shunt}).

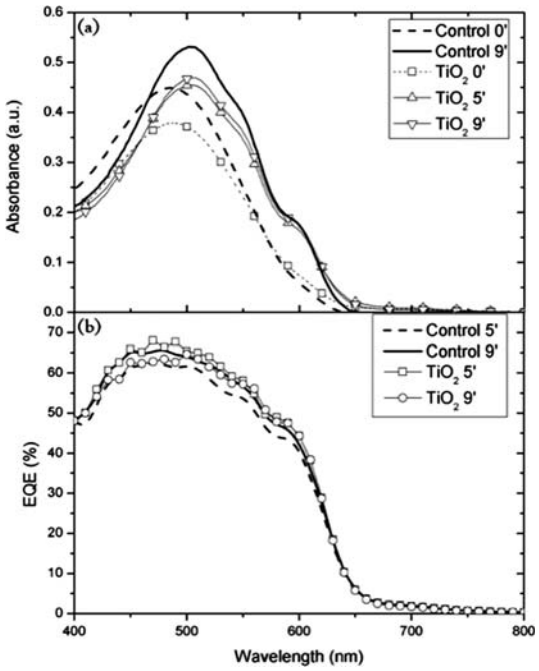

Fig. 5 (a) Comparison of absorption spectrum between devices with normal active layer and active layer with 0.002 mol per 100 mL TiO_2 nanotube. (b) External quantum efficiency (EQE) comparison between solar cell with and without TiO_2 nanotube aggregates annealed at 150 °C for different times.

~475 nm to ~550 nm, which is the main absorption range of P3HT. Meanwhile, only a slight increase in the spectra appears in the range from ~625 nm to ~675 nm. The drop of absorption in the range of 475–550 nm is assumed to be a result of less P3HT present in the device with TiO_2 nanotube aggregates occupying the space where P3HT would otherwise be. Except for this decrease in the main absorption range of P3HT, the absorption of TiO_2 nanotube aggregate containing devices behaves very similarly to the normal P3HT:PCBM devices during thermal treatment: after annealing at 150 °C, a red shift of the peak was seen in the absorption spectrum and shoulders at ~575 nm and 600 nm were distinguishable. However, from the values of short current density of devices (Table 1 and Fig. 4(a)), it can be seen that the amount of current produced did not change much before and after adding TiO_2 nanotube aggregates. As TiO_2 nanotube aggregate devices had lower absorbance and exciton separation is almost 100% in the P3HT:PCBM solar cell,[30] it was hypothesized that the TiO_2 nanotube aggregates help to improve the charge collection or transportation of the active layer and prevent geminate recombination.

Table 2 Electron mobility of active layer of devices with and without TiO_2 nanotube aggregates (derived from electron-only SCLC)

	μ_e/cm^2 V^{-1} s^{-1}	
Annealing time	5 min	9 min
Control	5.13×10^{-5}	5.71×10^{-5}
TiO_2	7.22×10^{-5}	6.72×10^{-5}

In order to test the hypothesis, further investigations were performed. Fig. 5(b) shows the external quantum efficiency of both P3HT:PCBM only devices and TiO_2 nanotube aggregate containing devices annealed for 5 min and 9 min. For the control group, the 9 min device had a higher EQE than the 5 min device due to the improved morphology obtained by annealing.[17] The EQE of both TiO_2 nanotube aggregate containing devices was very close to the 9 min control sample. Comparing this with their absorbance (Fig. 5), it confirms that even though the TiO_2 nanotube aggregate containing devices absorb less photons than the control devices, similar amount of charge carriers was collected in both devices. Consequently, the charge carrier collection was improved by adding TiO_2 nanotube aggregates.

The charge transportation ability of devices in both types was compared by measuring the electron-only space-charge-limited current (SCLC). The electron mobility of the active layer in each type (Table 2) was calculated by applying the method in ref. 31. It can be seen that by adding the TiO_2 nanotube aggregates the electron mobility of devices increases from 5.1×10^{-5} cm^2 V^{-1} s^{-1} to 7.2×10^{-5} cm^2 V^{-1} s^{-1} for device annealed for 5 min and from 5.71×10^{-5} cm^2 V^{-1} s^{-1} to 6.72×10^{-5} cm^2 V^{-1} s^{-1} for devices annealed for 9 min. This is consistent with device performance and morphology study of TiO_2 nanotube aggregate containing devices annealed for 5 min. We speculate that after annealing for 5 min, the region close to the TiO_2 nanotube aggregates achieved the optimal phase separation (Fig. 2(d)), which resulted in a larger population of electrons to be created that could be rapidly transported by the TiO_2 nanotube aggregates. At 9 min annealing time, although the rest of the film reached the optimal phase separation (Fig. 2(g)), morphology in the area adjacent to TiO_2 nanotube aggregates had already further separated (Fig. 2(f)). This caused less electrons to be created that were capable of being rapidly transported by the TiO_2 nanotube aggregates.

Conclusions

In conclusion, we have fabricated polymer solar cells based on P3HT:PCBM by adding TiO_2 nanotube aggregates into the active layer. Although the aggregates decreased the absorbance of device, they also improved the charge transportation and collection inside the active layer. Due to the presence of TiO_2 nanotube aggregates, different morphologies of active layer and optimal annealing condition were observed between the control device and TiO_2 containing devices. The power conversion efficiency of the devices reached as high as 3.2%, which corresponds to a 15% increase in PCE as a result of improved electron transport. We believe that this is a simple method that can be used to improve the efficiency of other polymer solar cells. But research on other factors of TiO_2 aggregates, such as the size, shape, crystal structure and arrangement, as well as TiO_2 concentration, is necessary to fully understand the whole picture of this system. We are currently investigating how the aggregates size, shape, and concentration can be changed to further improve the performance of OPVs.

Acknowledgements

This work has been supported by the DOE Solar America Initiatives Award (DE-FC36-08GO18024).

References

1 B. A. Gregg, *J. Phys. Chem. B*, 2003, **107**, 4688.
2 F. C. Krebs, *Sol. Energy Mater. Sol. Cells*, 2009, **93**, 394.
3 H. Hoppe and N. S. Sariciftci, *J. Mater. Res.*, 2004, **19**, 7.
4 F. C. Krebs, S. A. Gevorgyan and J. Alstrup, *J. Mater. Chem.*, 2009, **19**, 5442.
5 R. Tipnis, J. Bernkopf, S. Jia, J. Krieg, S. Li, M. Storch and D. Laird, *Sol. Energy Mater. Sol. Cells*, 2009, **93**, 1457.
6 S. Günes, H. Neugebauer and N. S. Sariciftci, *Chem. Rev.*, 2007, **107**, 1324.
7 B. C. Thompson and J. M. J. Fréchet, *Angew. Chem., Int. Ed.*, 2008, **47**, 58.
8 F. Padinger, R. S. Rittberger and N. S. Sariciftci, *J. Appl. Phys.*, 2006, **100**, 034907.
9 J. J. M. Halls, C. A. Walsh, N. C. Greenham, E. A. Marseglia, R. H. Friend, C. Moratti and A. B. Holmes, *Nature*, 1995, **376**, 498.
10 F. P. Rittberger, R. S. Rittberge and N. S. Sariciftci, *Adv. Funct. Mater.*, 2003, **13**, 85.
11 H. Hoppe and N. S. Sariciftci, *J. Mater. Chem.*, 2006, **16**, 45.
12 K. Sivula, Z. T. Ball, N. Watanabe and J. M. J. Fréchet, *Adv. Mater.*, 2006, **18**, 206.
13 W. Ma, C. Yang, X. Gong, K. Lee and A. J. Heeger, *Adv. Funct. Mater.*, 2005, **15**, 1617.
14 M. Hoppe, M. Niggemann, C. Winder, J. Kraut, R. Hiesgen, A. Hinch, D. Meissner and N. S. Sariciftci, *Adv. Funct. Mater.*, 2004, **14**, 1005.
15 C. W. Chu, H. Yang, W. J. Hou, J. Huang, G. Li and Y. Yang, *Appl. Phys. Lett.*, 2008, **92**, 103306.
16 G. Li, Y. Yao, H. Yang, V. Shrotriya, G. Yang and Y. Yang, *Adv. Funct. Mater.*, 2007, **17**, 1636.
17 G. Li, V. Shrotriya, Y. Yao and Y. Yang, *J. Appl. Phys.*, 2005, **98**, 043704.
18 M. Reyes-Reyes, K. Kim and D. L. Carroll, *Appl. Phys. Lett.*, 2005, **87**, 083506.
19 J. K. Lee, W. L. Ma, C. J. Brabec, J. Yuen, J. S. Moon, J. Y. Kim, K. Lee, G. C. Bazan and A. J. Heeger, *J. Am. Chem. Soc.*, 2008, **130**, 3619.
20 K. Shankar, G. K. Mor, M. Paulose, O. K. Varghese and C. A. Grimes, *J. Non-Cryst. Solids*, 2008, **354**, 2767.
21 G. K. Mor, K. Shankar, M. Paulose, O. K. Varghese and C. A. Grimes, *Appl. Phys. Lett.*, 2007, **91**, 152111.
22 T. Rattanavoravipa, T. Sagawa and S. Yoshikawa, *Sol. Energy Mater. Sol. Cells*, 2009, **92**, 1445.
23 D. C. Olson, J. Piris, R. T. Collins, S. E. Shaheen and D. S. Ginley, *Thin Solid Films*, 2006, **496**, 26.
24 H. E. Unalan, P. Hiralal, D. Kuo, B. Parekh, G. Amaratunga and M. Chhowalla, *J. Mater. Chem.*, 2008, **18**, 5909.
25 Y. Y. Lin, C. Chen, T. Chu, W. Su, C. Lin, C. Ku, J. Wu and C. Chen, *J. Mater. Chem.*, 2007, **17**, 4571.
26 M. Wang and X. Wang, *Sol. Energy Mater. Sol. Cells*, 2007, **91**, 1782.
27 Y. T. Lin, T. W. Zeng, W. Z. Lai, C. W. Chen, Y. Y. Lin, Y. S. Chang and W. F. Su, *Nanotechnology*, 2006, **17**, 5781.
28 C. C. Tsai and H. Teng, *Chem. Mater.*, 2006, **18**, 367.
29 Q. Zhang, T. P. Chou, B. Russo, S. A. Jenekhe and G. Cao, *Adv. Funct. Mater.*, 2008, **18**, 1654.
30 H. Ohkita, S. Cook, Y. Astuti, W. Duffy, S. Tierney, W. Zhang, M. Heeney, I. McCulloch, J. Nelson, D. D. C. Bradley and J. R. Durrant, *J. Am. Chem. Soc.*, 2008, **130**, 3030.
31 C. Goh, R. J. Kline, M. D. McGehee, E. N. Kadnikova and J. M. J. Fréchet, *Appl. Phys. Lett.*, 2005, **86**, 122110.

